J|A|C|S
COMMUNICATIONS

Published on Web 04/22/2003

Synthesis of Tin-Encapsulated Spherical Hollow Carbon for Anode Material in Lithium Secondary Batteries

Kyu T. Lee, Yoon S. Jung, and Seung M. Oh*

School of Chemical Engineering and Research Center for Energy Conversion & Storage, Seoul National University, Seoul, 151-744, Korea

Received February 7, 2003; E-mail: seungoh@plaza.snu.ac.kr

Metallic Sn has been projected as a promising anode material for lithium secondary batteries. Its theoretical specific capacity (992 mA h g^{-1}) is much higher than that of the already-commercialized graphite (372 mA h g^{-1}).[1] Even this, its commercial use is still hindered. The most critical problem in this material is the severe volume expansion/contraction during the alloying and dealloying reaction with Li^+ ions. Due to the volume change, Sn metal particles are pulverized to eventually lose its Li^+ storage ability.[2] To solve this problem, Sn metals were prepared in nanosize, and a partial improvement was achieved by reducing the absolute volume change.[3] A new problem was, however, encountered with nanosized materials whereby extremely small metal particles are aggregated to be larger particles during the alloying and dealloying reaction, then pulverized again.[4]

In this work, we tried to improve the cycle performance of nanosized Sn metal particles by encapsulating with spherical hollow carbon. The spherical hollow carbon plays several important roles in this preparation. First, the hollow carbon acts as a barrier to prevent the aggregation between Sn particles. Second, the hollow carbon provides a void space where Sn metal particles experience a volume change without a collapse of carbon shell. Third, the hollow carbon itself is an active material for additional Li^+ ion storage. Finally, the carbon particles are spherical in shape, which provides a high packing density in practical Li cells to allow a high volumetric energy density.

The synthetic procedure is summarized in Scheme 1. In detail, cetyltrimethylammonium bromide (CTAB, 0.246 mmol as a surfactant) was dispersed in deionized water (5.6 mol) to form spherical micelles. Then, the mixture of resorcinol (R, 1 mmol), formaldehyde (F, 1 mol), and sodium carbonate (0.014 mmol as a catalyst for RF sol−gel polymerization) was added to obtain surfactant-stabilized (templated) RF sols. Next, tributylphenyltin (TBPT, 1 mmol as a Sn source) was added to obtain surfactant-stabilized TBPT/RF core−shell colloids. This core−shell structure is made due to the hydrophilicity difference between TBPT and RF sol. That is, TBPT and RF sol is immiscible to each other. Furthermore, as TBPT is less hydrophilic than RF sol, TBPT is located inside RF sol that is in turn stabilized by the surfactant micelles in aqueous medium.[5] The RF sol was then polymerized at 85 °C to obtain the TBPT-encapsulated RF polymer (Figure 1a). After drying in a convection oven, the product was heat-treated at 700 °C for 2 h under argon atmosphere to carbonize the RF polymer. During the heat treatment, the RF polymer was carbonized to spherical carbon shell, whereas TBPT decomposed into nanosized Sn metal that was melted and then deposited inside the hollow carbon shell (Figure 1b). The void space was generated by the decomposition of TBPT (Figure 1b). The pore size distribution that was calculated by the Barrett−Joyner−Halenda (BJH) method from the adsorption branch of nitrogen isotherm reveals that this material contains macropores (>100 nm) and mesopores (2 nm). The macropores represent the cavity size of hollow carbon, and this is consistent with the TEM image (Figure 1b). The mesopores are seemingly generated during the carbonization of RF polymer. In this particular synthesis, the Sn content in the composite was 24 wt % that was estimated from

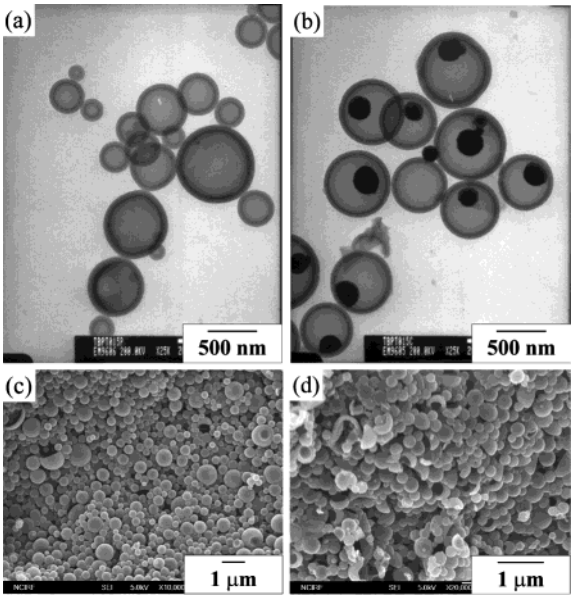

Figure 1. Transmission electron micrograph of the core−shell structure of tributylphenyltin/RF polymer (a) and Sn-encapsulated spherical hollow carbon. (b) Field-emission scanning electron micrograph of TC1 (c) and TC2 (d). The images were obtained with JEOL JEM 2000 EXII and JSM 6700F, respectively.

Scheme 1. Synthetic Scheme for Sn-Encapsulated Spherical Hollow Carbon

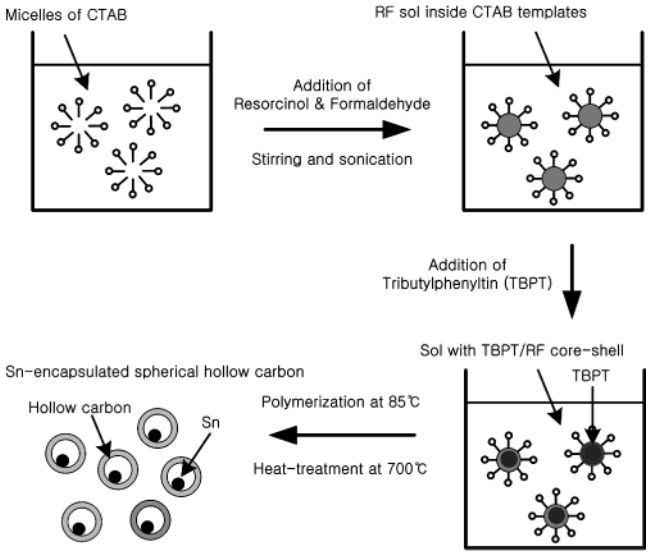

10.1021/ja0345524 CCC: $25.00

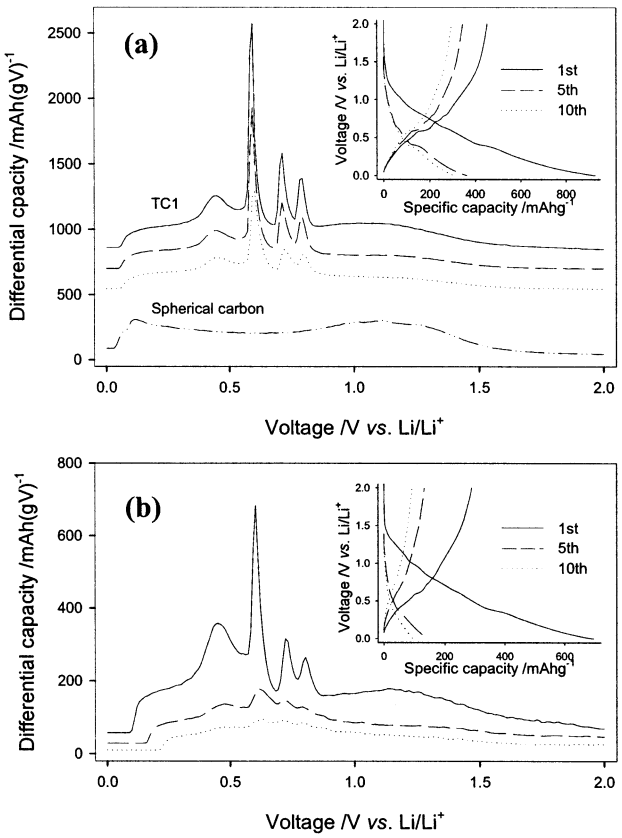

Figure 2. The differential discharging capacity profiles taken with TC1 (a) and mixture electrode (b). The galvanostatic charge−discharge voltage profiles are provided in the inset.

the thermogravimetric analysis made in air atmosphere. The formation of β-Sn was confirmed by the X-ray diffraction analysis.

In this preparation, the size of spherical hollow carbon can be controlled by the resorcinol/surfactant ratio with the other variables being fixed. When the mole ratio of R/CTAB was reduced from 4.1 (TC1) to 2.4 (TC2), the size of carbon spheres decreased from ca. 1 to ca. 0.5 μm as shown in the field emission scanning electron microscopy (FE-SEM) images (Figure 1, c and d). This is possible because a smaller amount of resorcinol is located in each micelle. The size of Sn metal was also controllable by varying the TBPT/CTAB mole ratio. Each micelle contains a less amount of Sn precursor when the TBPT/CTAB ratio becomes smaller.

Figure 2 compares the cycle performance for TC1 electrode and a mechanical mixture of 100 nm-sized Sn metal (Alfa Aesar) and 100 nm-sized spherical carbon.[6] The size effect of Sn metal can be ignored because the size of Sn metal in the mixture electrode is comparable to that of Sn inside TC1. The spherical carbon was synthesized at the same conditions for TC1 without TBPT. The differential discharging capacity profiles that were derived from the discharge voltage profiles shown in the inset indicate that both Sn and carbon are participating in the reaction with Li^+ ions. The profile taken with the spherical carbon is provided in Figure 2a for reference. Four separate peaks at 0.4−0.8 V are related with the dealloying reaction of Sn component,[7] whereas the broad background corresponds to the Li^+ removal from the carbon. The discharge capacity delivered by the Sn component is, however, far different for two electrodes. The Sn component in the mixture electrode shows a rapid capacity fade as seen in Figure 2b, whereby a disappearance of Sn-related peaks within 10 cycles is noticed. The peaks at 0.4−0.8 V are still quite intense in the case of TC1 electrode even after 10 cycles, indicative of a better capacity retention of Sn component. It is likely that the aggregation and pulverization of nanosized Sn metal particles is suppressed by encapsulating with the hollow carbon shell.

TC1 electrode as well as the mixture electrode suffers from an irreversible capacity loss in the first cycle that is largely come from the electrolyte decomposition on carbon surface.[8] The surface area of spherical carbon was 399 $m^2\ g^{-1}$. Accordingly, the TC1 electrode exhibits a Coulombic efficiency of 49% in the first cycle, but more than 90% from the second cycle. The discharge capacity of TC1 electrode amounts to 452 mA h g^{-1} in the first cycle when discharged from 0.0 to 2.0 V with a current density of 50 mA g^{-1}. By subtracting the capacity of spherical carbon (373 mA h g^{-1}) that was separately measured, the discharge capacity delivered by the Sn component (24 wt %) was estimated to be 169 mA h. From this, the specific capacity of Sn in the TC1 electrode was calculated to be 704 mA h g^{-1}, which amounts to about 70% of the theoretical value (992 mA h g^{-1}).

Acknowledgment. This work was supported by KOSEF through Research Center for Energy Conversion and Storage. A financial support from Samsung SDI Co. is also acknowledged.

Supporting Information Available: TGA result of TC1 and TC2, XRD patterns of Sn-encapsulated hollow carbon and tributylphenyltin/RF polymer, nitrogen adsorption−desorption isotherm and pore size distribution of TC1, and charge/discharge capacity profiles according to cycle number (PDF). This material is available free of charge via the Internet at http://pubs.acs.org.

References

(1) (a) Idota, Y.; Kubota, T.; Matsufuji, A.; Maekawa, Y.; Miyasaka, T. *Science* **1997**, *276*, 1395−1397. (b) Winter, M.; Besenhard, J. O.; Spahr, M. E.; Novak, P. *Adv. Mater.* **1998**, *10*, 725−763. (c) Wang, J.; Raistrick, I. D.; Huggins, R. A. *J. Electrochem. Soc.* **1986**, *133*, 457−460. (d) Goward, G. R.; Leroux, F.; Power, W. P.; Ouvrard, G.; Dmowski, W.; Egami, T.; Nazar, L. F. *Electrochem. Solid-State Lett.* **1999**, *2*, 367−370.

(2) (a) Beaulieu, L. Y.; Eberman, K. W.; Turner, R. L.; Krause, L. J.; Dahn, J. R. *Electrochem. Solid-State Lett.* **2001**, *4*, A137−A140. (b) Peng, Z.; Shi, Z.; Liu, M. *Chem. Commun.* **2001**, 2125−2126. (c) Fransson, L.; Nordström, E.; Edström, K.; Haggström, L.; Vaughey, J. T.; Thackeray, M. M. *J. Electrochem. Soc.* **2002**, *149*, A736−A742. (d) Veeraraghvan, B.; Durairajan, A.; Haran, B.; Popov, B.; Guidotti, R. *J. Electrochem. Soc.* **2002**, *149*, A675−A681.

(3) (a) Li, H.; Wang, Q.; Shi, L.; Chen, L.; Huang, X. *Chem. Mater.* **2002**, *14*, 103−108. (b) Limthongkul, P.; Wang, H.; Jud, E.; Chiang, Y. *J. Electrochem. Soc.* **2002**, *149*, A1237−A1245. (c) Li, N.; Martin, C. R. *J. Electrochem. Soc.* **2001**, *148*, A164−A170.

(4) (a) Courtney, I. A.; McKinnon, W. R.; Dahn, J. R. *J. Electrochem. Soc.* **1999**, *146*, 59−68. (b) Li, H.; Shi, L.; Lu, W.; Huang, X.; Chen, L. *J. Electrochem. Soc.* **2001**, *148*, A915−A922.

(5) (a) Tiarks, F.; Landfester, K.; Antonietti, M. *Langmuir* **2001**, *17*, 908−918. (b) Loxley, A.; Vincent, B. *J. Colloid Interface Sci.* **1998**, *208*, 49−62.

(6) The galvanostatic charge/discharge cycling was made with a three-electrode cell, where Li metal foil was used as the counter and reference electrode. The used electrolyte was 1.0 M $LiClO_4$ dissolved in a mixture of ethylene carbonate and diethyl carbonate (1:1, v/v). For the preparation of TC1 and mixture electrode, the slurry made with active material, conducting agent (Super P) and poly(tetrafluoroethylene) (10:1:1, weight ratio) was coated on a piece of copper exmet (apparent area = 1 cm^2). The molded electrodes were then dried at 120 °C under vacuum for 12 h. For the galvanostatic charge/discharge cycling, a gravimetric current density of 50 mA g^{-1} was applied within a voltage range of 0.0−2.0 V (vs Li/Li^+). All the electrochemical measurements were carried out at 25 °C.

(7) (a) Ulus, A.; Rosenberg, Y.; Burstein, L.; Peled, E. *J. Electrochem. Soc.* **2002**, *149*, A635−A643. (b) Beaulieu, L. Y.; Beattie, S. D.; Hatchard, T. D.; Dahn, J. R. *J. Electrochem. Soc.* **2003**, *150*, A419−A424.

(8) (a) Zaghib, K.; Nadeau, G.; Kinoshita, K. *J. Electrochem. Soc.* **2000**, *147*, 2110−2115. (b) Chung, G. C.; Jun, S. H.; Lee, K. Y.; Kim, M. H. *J. Electrochem. Soc.* **1999**, *146*, 1664−1671. (c) Kwon, K.; Kong, F.; McLarnon, F.; Evans, J. W. *J. Electrochem. Soc.* **2003**, *150*, A229−A233.

JA0345524